Structural analysis of the Eola – Robberson Field using balanced cross sections, Garvin County, Oklahoma

Derya Kilic[1] and Bryan Tapp[2]

[1]Department of Geosciences, The University of Tulsa, 800 S. Tucker Drive, Tulsa, Oklahoma, 74104. Current Address: Turkiye Petrolleri A.O. Sogutozu Mahallesi, 2180. Cadde, No:86, 06100, Cankaya-Ankara, Turkiye. dkilic@tpao.gov.tr.
[2]Department of Geosciences, The University of Tulsa, 800 S. Tucker Drive, Tulsa, Oklahoma, 74104. jbt@utulsa.edu. Corresponding author.

ABSTRACT

A detailed subsurface structural analysis was undertaken in the Eola – Robberson Field, Garvin County, Oklahoma, USA, to characterize its structural style. Eola – Robberson is near the boundaries of three key tectonic elements in the Southern Oklahoma Aulacogen. The field is at the junction of the Arbuckle Uplift, the Anadarko Basin and the Ardmore Basin. The field is structurally complex and multiple styles and modes of deformation had been previously suggested. No balanced cross sections had been developed in the field. Based on detailed log analysis, three cross sections were balanced with an average error of less than 2% using line length and kink-bed methods. The results suggest transpressional deformation with significant vertical uplift. The amount of shortening in the cross sections varies from 32% at the western end of the field to 53% near the eastern end of the field. Three major faults in the field have significant vertical uplift, displacing basement from approximately 14,000 ft (4,267 m) subsea to 1,000 ft (305 m) subsea in the central pop-up feature in the field. The central block is continuous throughout the field. Based on this research we interpret the field as a transpressional feature.

The main faults in the field may represent the original rift-bounding faults of the Southern Oklahoma Aulacogen that were reactivated by contraction and wrenching during the Wichitan and Arbuckle orogenies. The exercise of balancing the cross sections gave insight into the geometry of faulting in the area. Further research is needed to determine total offsets. The work has significant implications for the original configuration of faults and the structural evolution of the Southern Oklahoma Aulacogen.

INTRODUCTION

This work is a continuation of research to characterize the structural style in the Southern Oklahoma Aulacogen, specifically, to examine the structural styles of oil fields near the fault boundaries of the Ardmore Basin. The basin has been shown to have a range of convergence angles on major faults, with convergence angles ranging from 10° in the Eola – Robberson Field to greater than 80° in the Velma Field (Granath, 1989). Previous studies have examined the structural style of the Milroy Field (Harmon and Tapp, 2001; Harmon et al., 2002), and the Sho-Vel-Tum (Simpson-Carpenter, 2011; Carpenter and Tapp, this guidebook) to describe the fault geometries and structural style of these fields. The objective of this study is to analyze the structural style in the Eola – Robberson Field using traditional, detailed subsurface mapping techniques and to determine if cross sections in the field can be geometrically balanced.

The Eola – Robberson Field is located in the southern part of Garvin County, Oklahoma, and may constitute the buried western extension of the Arbuckle system (Figure 1). The field was discovered in 1945 with production from the basal Bromide sandstone (Swesnik and Green, 1950). The field has an estimated ultimate recovery of 213 MMBO (Henry and Hester, 1995). The principal product of Eola – Robberson Field is oil, with production from the Simpson Group (basal Oil Creek sandstone, basal McLish sandstone, basal Bromide sandstone, upper Bromide sandstone, Bromide dense limestone), Viola Limestone, Hunton limestone, Woodford Shale, Sycamore Limestone, and the Eola conglomerate (McCaskill, 1998).

An understanding of the field is significant in that it lies near the boundaries of the Arbuckle Uplift, the Ardmore Basin and the Anadarko Basin (Figure 2). These are key elements of the Southern Oklahoma Aulacogen.

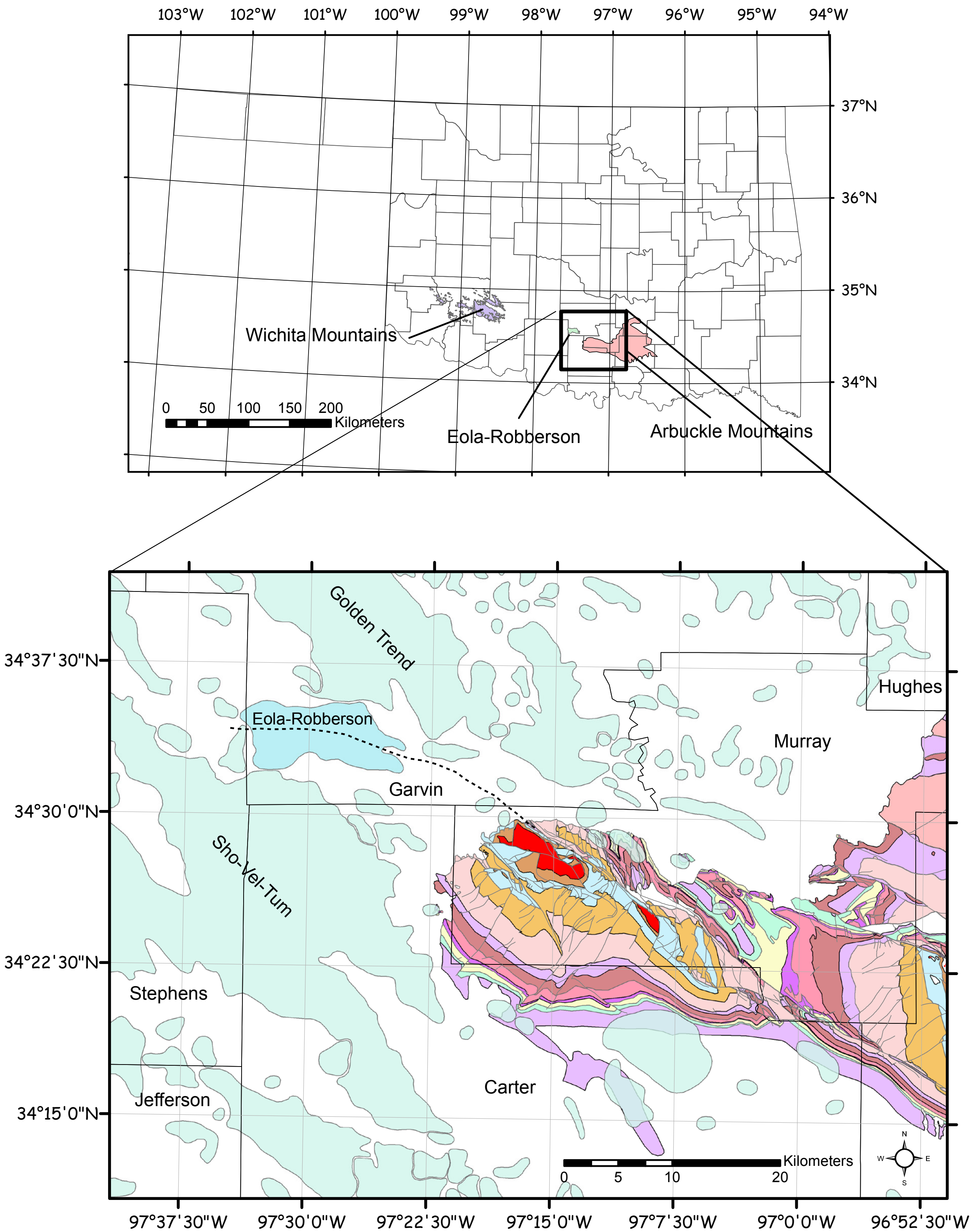

Figure 1: Location map of the Eola – Robberson Field shown relative to Arbuckle Uplift. Digital data from Cederstrand (1996), and Boyd (2002). The subsurface continuation of the Washita Valley Fault (dashed) is modified from Booth (1981).

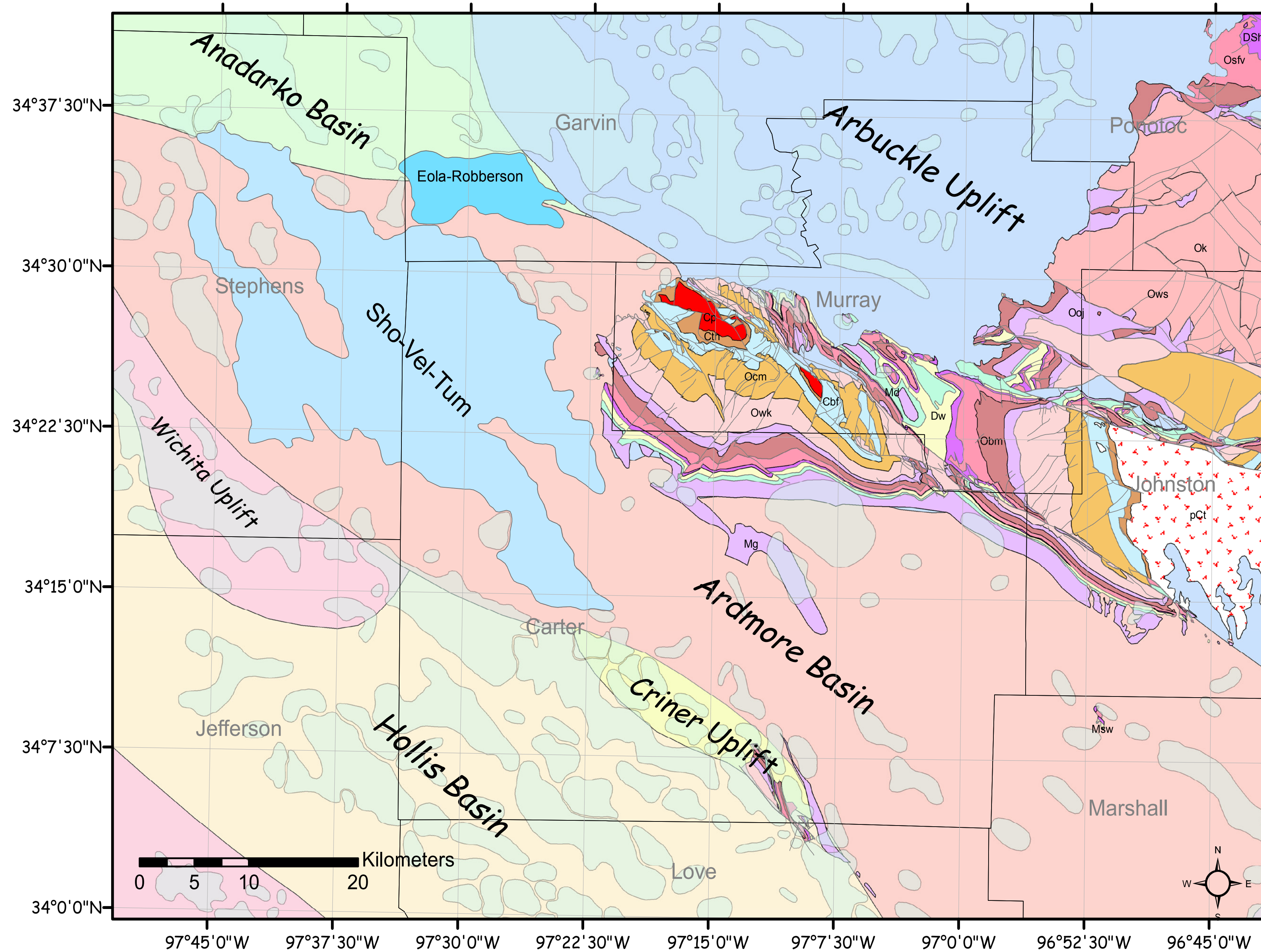

Figure 2: Relationship of Eola – Robberson Field to major tectonics elements of the Southern Oklahoma Aulacogen. The Field is near the boundaries of the Arbuckle Uplift, Ardmore Basin and Anadarko Basin. Digital data from Northcutt and Campbell (1995); Cederstrand (1996), and Boyd (2002).

Logs from more than 250 wells were examined in detail to pick formation tops in the Ordovician to Pennsylvanian section (Figure 3). These wells were used to prepare subcrop maps, structural contour maps and cross sections. Three cross sections were balanced by the line-length and kinked-bed methods (Suppe, 1983; Mount, et al., 1990) to validate the geometry of the structural interpretations.

The Eola – Robberson Field is controlled by west-northwest trending structures (Harlton, 1964). The Washita Valley Fault is considered the major controlling structural element in the area that borders the Eola Field to the south (Harlton, 1964; McCaskill, 1998).

The Eola – Robberson Field is structurally complex. This complexity has lead to a wide range of interpretations. Phillips (1983) interpreted gravity slide blocks in the Eola, Southeast Hoover, and Southwest Davis Oil Fields and in the western Arbuckle Mountains. Brownlee (1985) interpreted the Eola structure as a klippe, suggesting that the system was a nappe feature that was transported into its current location through wrench faulting. McCaskill (1998) provided a detailed analysis of the stratigraphy of the field and concluded that there was as much as 16 miles (26 km) of left-lateral displacement on the fault. The variation of interpretation of structural style in the Eola – Robberson Field mirrors the discussion of evolution of and structural style in the Arbuckle system. Authors working in the region have interpreted the structural style as pure thrusting (Brown, 1984; Dott, 1934), strike-slip (Booth, 1981; Carter 1979), transpression (Granath, 1989; Simpson-Carpenter, 2011), and inversion (Tapp, 1995). Given the disparate interpretations for the structural style of the field, this study seeks to provide a description of the structural geology and to prepare detailed cross sections based on geological data gathered through classical subsurface mapping techniques.

Methods

Over 2200 wells in T1N-R3W and T1N-R2W (Eola – Robberson Field) were imported into a PETRA® project for study. The number of wells for detailed subsurface analysis was reduced to approximately 250 based on location, formation at TD, age of the well, and quality and raster log type. The well data provided by IHS includes API numbers, name, location, azimuth/dip and condition of the well, and formation tops. Raster images of logs were obtained from MJ Systems. The log suites included gamma ray, caliper, induction, laterolog, resistivity, density, neutron, SP, sonic, PE, and dipmeter. Not all log types were available for each well.

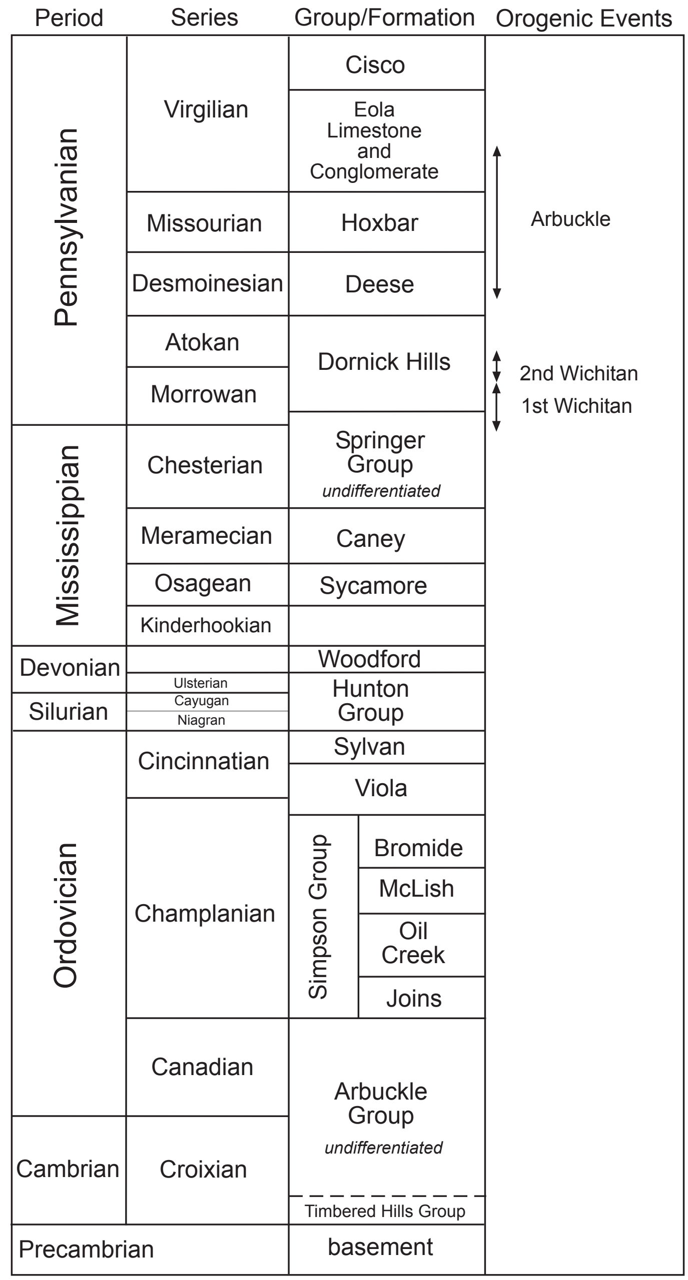

Figure 3: Generalized composite stratigraphic chart (modified from Granath (1989) and Boyd (2008)).

The stratigraphic section beneath the Pennsylvanian unconformity was studied in this project. Springer, Caney, Sycamore, Woodford, Hunton, Sylvan, Viola, Bromide, McLish, Oil Creek, and Arbuckle tops were picked throughout the study area. Correlation markers were based on extensive log study and are listed in Table 1 with an indication of confidence in the pick. Formation tops that were of high confidence and consistent through the study

TABLE 1. LOG RESPONSES FOR STRATIGRAPHIC PICKS USED IN THIS STUDY.

LOG RESPONSES FOR FORMATION TOPS			
			Based on wells: API # 35-049-21665-0000 & #35-049-22770-0000
FORMATION	IHS-TOPS	CI	DESCRIPTION
SPRINGER	401-SPRG	H	Shale interval with 75-90 API gamma ray values, Resistivity nearly constant at 2-3 ohms.m2/m
CANEY	354-CNEY	H	GR increase up to 135 API, Resistivity increases, include hot shale int. before Caney shale resistivity is constant at 2-3 ohm.m, slight increase in SP
SYCAMORE	319-SCMR	M	Resistivity increase, include sand-shale intervals with change in GR, resistivity increases at sand intervals
WOODFORD	319-WFDD	H	GR > 150 API including off-scale hot shale int, resitivity nearly constant at 2000.0 ohm.m, no change in SP
HUNTON	269-HNTN	H	Top of limestone, GR between 30-45 API, higher resistivity at base and top, include sandy limestone
SYLVAN	203-SLVN	H	Top of shale, GR between 105-120 API, SP increase slightly, resistivity icreases at last 80 feet, sharp contact in resistivity and very thin hot shale unit at base
VIOLA	202-VIOL	H	Top of limestone,GR between 15-30 API, @ middle viola GR increase slighly, res constant at 2000.0 ohms.m2/m
GR-DN-8	202-BMDD	H	Thin, consistent shale int (~5') with increase in GR, resistivity decrase sharply from 2000.0 to 150.0 ohms.m2/m
GR-DN-7	_	M	Shale interval bounded by limestone int, GR increase up to 105 API, resistivity decreases.
GR-DN-6	BRMD-3	M-L	Base of shaly interval with GR kicks and neutron porosity increase, not significant in resistivity curve
GR-DN-5	_	L	Base of shaly interval (nearly 40' in thickness), not significant in resistivity curve
GR-DN-4	202-MCLS-L	M	Top of sandstone-nearly 100' in thickness from neutron-density curve, GR around 15-30 API, res decrease to 20.0 probably this sandstone is the base of the McLish.
OILCREEK	202-OLCK	H	Top of shale, GR starts with 120 API and decrease to 30 towards the base, shale dominant,sandy, limestone int. more sandy at base
GR-DN-2	202-OLCK-L	M	Top of sandstone int from DN, GR value between 15-30 API, resistivity decrease to 20.0, basal OLCK sandstone?
GR-DN-1	202-JOINS	H	Base of sandstone, GR increase to 75 API, limestone, dolomite int below sandstone,

area were selected to develop cross sections. Additional log signatures (stratigraphic sub-units based on consistent log character) were used for local correlation in complex areas. Any missing stratigraphic intervals due to unconformities or faulting were noted. Similarly, repeated stratigraphic intervals and any overturned sections were noted.

Initially, seven structural cross sections that cross the field in a general southwest to northeast direction were constructed (Kilic, 2013). Three of these cross sections were balanced by line-length and kinked-bed methods (Mount et al., 1990; Suppe, 1983;). Balanced cross sections are used to determine if a cross section is geometrically acceptable and to determine the original undeformed length and shortening in a cross section (Mitra, 1992). In balancing, deformed beds are flattened and returned to their original depositional position (Dahlstrom, 1969; Mitra, 1992). When beds can be restored, the cross section is geometrically acceptable. In using these methods, we assumed uniform bed thickness and length as well as angular fold and fault geometries (Dahlstrom, 1969; Suppe, 1983). It is important to note that a balanced cross section is geometrically acceptable, and may be considered a reasonable geometry of the current fault configuration. In areas of significant lateral deformation, the cross sections will not provide a kinematic model of faulting or an indication of total displacement (Dewey et al., 1998).

In the line-length method, a vertical pin-line is placed in the most undisturbed part of the section (Geiser, 1988; Mitra, 1992; Woodward, et al., 1985). Bed lengths of selected layers are measured, fault contacts are marked and beds are flattened to their initial undeformed position from the pin-line (Dahlstrom, 1969; Mitra, 1992). A balanced cross section shows consistent bed lengths and trajectories of faults (Mitra, 1992). Balancing is an iterative process that is repeated with differing geometries until there is reasonable error (5% or less) in the balanced section.

The kinked-bed method is geometrically straightforward because kink folds have straight limbs and angular hinges (Suppe, 1983). In this method, all beds are assumed to have a kink-fold geometry with the length and thickness of beds preserved (Mitra, 1992). For this project, the three cross sections were balanced with less than 2% error.

Results

As part of the initial study, a series of subcrop maps were prepared at 1,000 ft (304 m) depth intervals from 1,000 to 9,000 ft (304 to 2,743 m) subsea (Kilic, 2013). These maps were used to help prepare a model of the fault system in the area and served as a basis for the location and preparation of the cross sections. The fault map corresponding to a subsea depth of approximately 2,000 ft (610 m) is shown in Figure 4. This map also shows the locations of the balanced cross sections. The Eola – Robberson Field is dominated by west-northwest striking faults and fault-related folds. Several repetitions in stratigraphy were observed in logs along the major faults, suggesting reverse faulting. These faults were labeled in order of their importance - whether they were present in all cross sections. Fault 1, Fault 2, and Fault 3 are continuous across the field and are interpreted as major reverse faults. Fault 4 is a splay of Fault 2 and occurs only in cross section A-A'. Fault 5 is interpreted as a normal cross-fault that occurs only in cross section A-A'. Fault 6 is a splay of Fault 3 occurring only in cross section C-C'. Faults 7, 8, and 9 occur only in cross section F-F'. Faults 8 and 9 merge in Sec. 2 T1N-R3W and then further merge with Fault 1 in Sec. 3, suggesting an anastomosing fault geometry. Faults that removed section were noted in several logs. These were interpreted as normal faults and mapped as shown in Figure 4. These normal cross-faults have a southwest-northeast strike and suggest a component of extension associated with the stucture of the field.

Balanced Cross Sections

Three cross sections were balanced using line-length and kink-bed restoration methods (Suppe, 1983; Mount et al. 1990). Cross sections were developed starting in the western part of the field where the fault geometries are simplest. The facing direction of the sections is toward the southeast along the strike of the major faults and down-plunge of the major fold in the field. In the cross sections, north is to the left, south is to the right. In each case, the basinward section of the system is to the right. This perspective is non-traditional, but was chosen to give the perspective of looking toward the Arbuckle Uplift. The locations of balanced cross sections A-A`, C-C`, and F-F` are shown in Figure 4. In each of the cross sections, depths are registered to sea level. The logs used in each cross section are identified by API Number and name in Table 2. A generalized line of profile is drawn at an elevation of 1,000 ft (304 m). The topographic relief in the area is minor, with a maximum elevation change of 157 ft (48 m) occurring along cross section A-A'.

Cross section A-A'

Cross section A-A` (Figure 5) is the westernmost cross section in the Eola – Robberson Field. The cross section

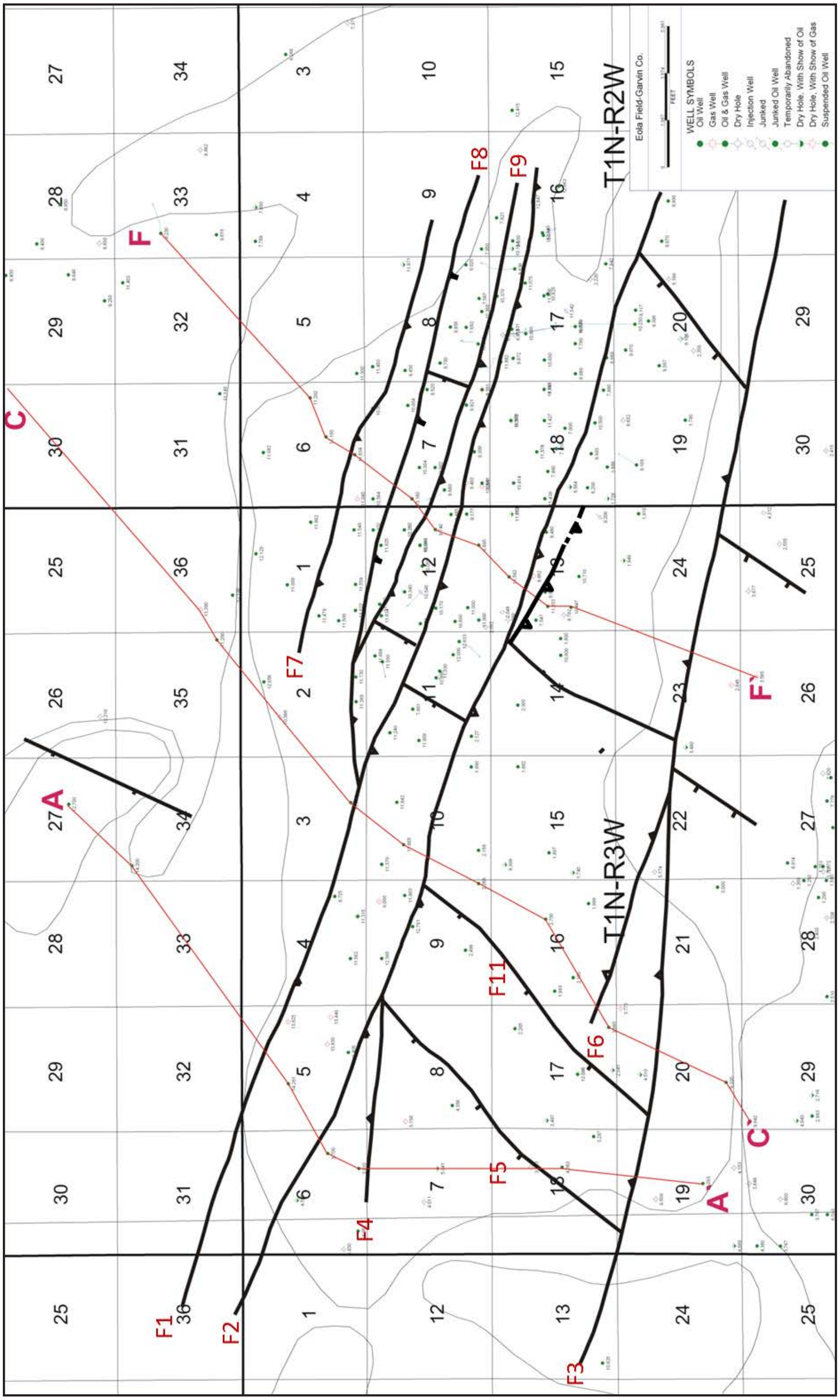

Figure 4. Composite fault map of Eola – Robberson Field showing location of balanced cross sections.

TABLE 2. API NUMBERS AND WELL INFORMATION FOR LOGS USED IN CONSTRUCTING THE BALANCED CROSS SECTIONS.

A-A' Cross Section				
No.	**API**	**Well Name and Number**	**Township-Range-Section**	**TD (ft)**
1	35049009410000	LULA C CASON #*1*	T2N-R3W-S27	12,700
2	35049226700000	FERGUSON #1	T2N-R3W-S34	14,200
3	35049000790000	JOHNSON #1	T1N-R3W-S5	14,261
4	35049364090000	D COLE #1	T1N-R3W-S6	3,700
5	35049364170000	G L ROSE #7	T1N-R3W-S26	3,610
6	35049363980000	PERKINS #1	T1N-R3W-S7	5,041
7	35049373150000	DERDEYN #1	T1N-R3W-S18	4,383
8	35049207490000	LANTON-THOMPSON #1	T1N-R3W-S19	10,093
C-C' Cross Section				
No.	**API**	**Well Name and Number**	**Township-Range-Section**	**TD (ft)**
1	35049228120000	OLIN #1-30	T2N-R2W-S30	9,119
2	35049212650000	EWERT #2-36	T2N-R3W-S36	13,390
3	35049213360000	POTTS #1-35	T2N-R3W-S35	11,200
4	35049009140000	HOUSE #1	T1N-R3W-S2	10,996
5	35049218780000	FERGUSON #*1-3*	T1N-R3W-S3	11,916
6	35049211010000	LEVY #2	T1N-R3W-S10	11,865
7	35049234450000	PERNELL THOMAS #20	T1N-R3W-S9	2,268
8	35049353840000	P W RICHARDSON #11	T1N-R3W-S16	2,700
9	35049237510000	PATSY #1-17	T1N-R3W-S17	3,980
10	35049210150001	MEINDERS *1-20*	T1N-R3W-S20	9,335
11	35049207230000	M DERDEYN #1	T1N-R3W-S29	9,042
F-F' Cross Section				
No.	**API**	**Well Name and Number**	**Township-Range-Section**	**TD (ft)**
1	35049246930000	HARWELL #1-33	T2N-R2W-S33	9,230
2	35049213820000	TALIFERRO #2-6	T1N-R2W-S6	11,292
3	35049219600000	FERGUSON #10-6	T1N-R2W-S6	11,150
4	35049365910000	FERGUSON B#1	T1N-R2W-S6	11,634
5	35049365820000	HARRELL C #2	T1N-R2W-S7	10,180
6	35049600330000	HARRELL 'B' #5-12	T1N-R3W-S12	9,740
7	35049242130000	COOK ELLA 'B' #5-12	T1N-R3W-S12	6,895
8	35049245560000	CHINCHILLA #1-13	T1N-R3W-S13	11,582
9	35049247580000	FERGUSON #2-13	T1N-R3W-S13	11,853
10	35049204150000	SPARKS UNIT 'B' #1	T1N-R3W-S13	10,447
11	35049246760000	HICKS #1	T1N-R3W-S26	3,585

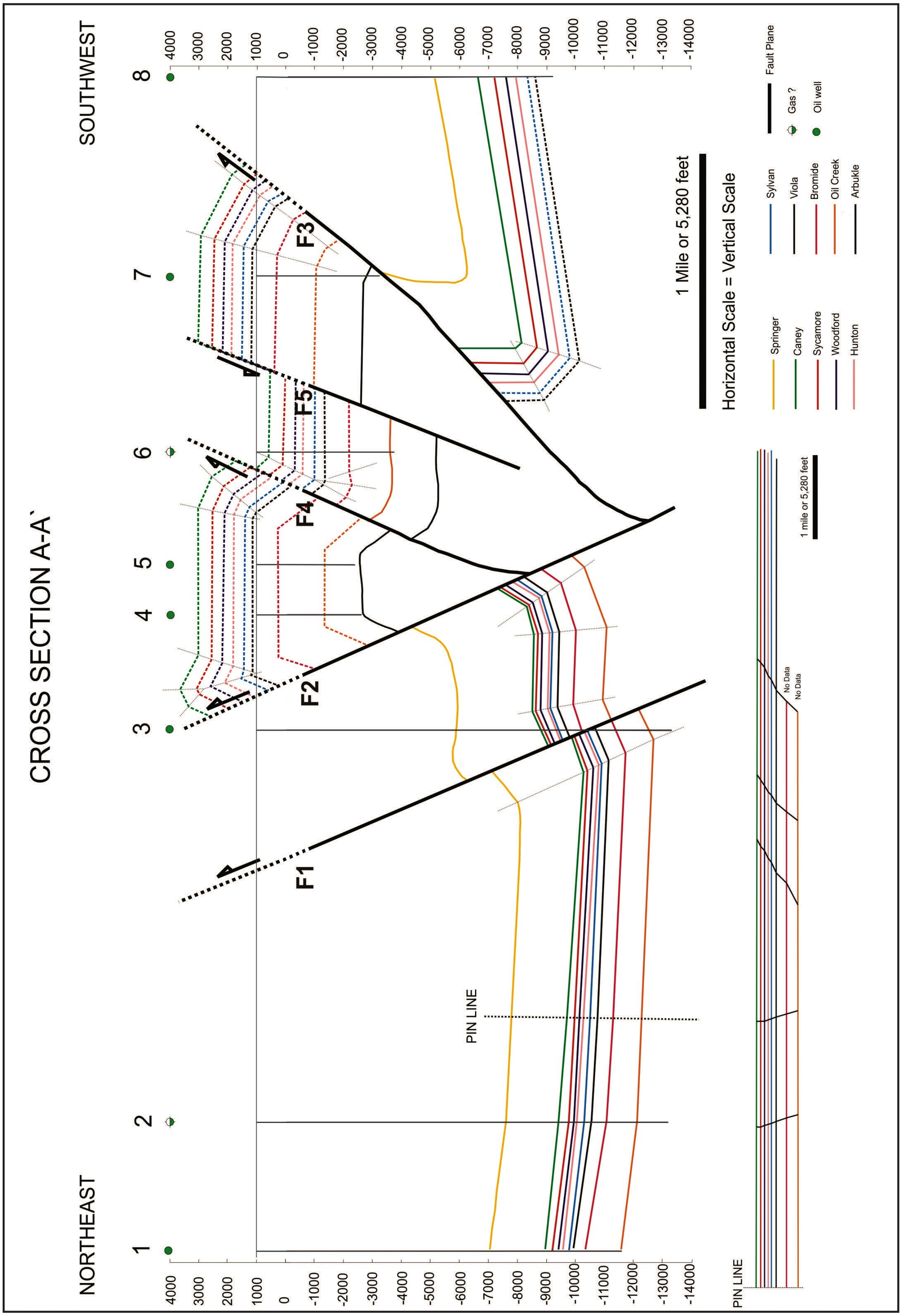

Figure 5. Cross Section A-A`. API and well information can be found in Table 2.

was constructed using eight wells. This cross section is balanced with Caney, Sycamore, Woodford, Hunton, Sylvan, and Viola tops flattened to an undeformed position. Each of the logs used in the cross section is shown as the vertical line corresponding to the well. The pin-line is located between Well 2 and Well 3 where the units are relatively undisturbed. This cross section balanced with 1.2% line length error. The total shortening in the section is 32 %. Fold geometries are interpretive in areas of limited log control and are generated using kink-bed methods.

The Springer Group to Oil Creek sandstone dip gently southwest with relatively constant interval thicknesses in the northern (left) part of the cross section. The first fault (Fault 1) in this cross section is a reverse fault that repeats ~900 ft (274 m) of the Bromide through Sylvan.

Fault 2 is interpreted as the main reverse fault in the field with significant vertical offset between Fault 2 and Fault 3. The approximate depth of the Arbuckle Group is more than 12,000 ft (3,658 m) subsea in the northern part of the field (Wells 1, 2 and 3). Between Fault 2 and Fault 3, the subsea depth of the Arbuckle top is as shallow as 2,300 ft (700 m). The net offset of the fault can only be approximated. The Arbuckle is truncated by the Pennsylvanian unconformity between Fault 2 and Fault 4 and again between Fault 5 and Fault 3. The approximate vertical separation on Fault 2 is about 9,700 ft (2956 m).

The area between Faults 2 and 3 is interpreted as a composite pop-up structure or positive flower structure (Harding, 1990). The eroded section between these reverse faults is represented as a series of dotted lines in the cross section. Faults are projected upward to the point where the complete stratigraphic section can be restored. Eroded parts of the section are depicted as dashed lines; these are used in the balancing process. Fault 4 is interpreted as a reverse fault dipping northeast. Fault 5 is interpreted as a normal cross fault dipping northeast and causing approximately 1,500 ft (457 m) of displacement of the Arbuckle Group and Oil Creek sandstone. Between Fault 4 and Fault 5, the Oil Creek subcrops below the Pennsylvanian unconformity.

Cross section C-C'

Cross section C-C` (Figure 6) was constructed using eleven wells (Table 2). The cross section is balanced with Caney, Sycamore, Woodford, Hunton, Sylvan tops flattened to an undeformed state. The pin-line in this cross section is located between Well 1 and 2. This cross section balanced with 1.5% error and the total shortening is 44%.

In the northeastern part of the cross section, the Springer to Oil Creek sequence dips gently south with nearly uniform interval thicknesses. Fault 1 is interpreted as being continuous between A-A' and this cross section. The amount and style of displacement on the fault is the same between the cross sections. Fault 2 is a major reverse fault and is interpreted as the major fault in the field. The region between Fault 2 and Fault 3 shows significant vertical displacement of the lower Paleozoic section with vertical separation of more than 11,000 ft (3353 m). Between Fault 2 and Fault 6, Arbuckle Group strata are overlain unconformably by Pennsylvanian sediments. Between Fault 6 and Fault 3, the Oil Creek subcrops beneath the unconformity. Fault 6 is interpreted as a backthrust to Fault 2 that formed as a room accommodation feature. The geometry of the faults is interpreted as a large-scale pop-up or positive flower structure (Harding, 1990).

Cross section F-F'

Cross section F-F` (Figure 7) was constructed using eleven wells (Table 2). The pin-line is located between Well 1 and 2. The cross section was balanced with the Caney, Sycamore, Woodford, Sylvan and Viola Formations flattened to an undeformed position. This is the most complex, and hence most interpretive, of the balanced cross sections.

The pre-Pennsylvanian section dips gently southwest north of Fault 7. Fault 7 shows minor reverse displacement of the section. Fault 8 removes Caney and Sycamore from Well 5 and is interpreted as locally having minor normal offset.

Fault 9 shows a complex repeat of the Sycamore in Well 6 with two closely spaced faults in the logs. In this cross section, Fault 1 and Fault 9 form a small-scale pop-up feature. Fault 2 and Fault 3 raise the Arbuckle, Reagan, and basement rocks to a depth of 1000 ft (305 m). This feature is interpreted as the major pop-up (positive flower structure) in the field (Harding, 1990). The most complex part of the cross section is a large overturned syncline between Faults 1 and 2. This interpretation is supported by the log in Well 9 (Ferguson #2-13) where the well penetrates, in succession from shallowest to deepest, Arbuckle, Reagan, basement, Reagan, basement, and an overturned sequence of Viola, Sylvan, Woodford, and Sycamore followed by a normal section of Woodford, Hunton, Sylvan with TD in the Viola. Hunton was not recognized in the overturned section and may be locally faulted out (not shown at this scale). Cross section F-F` balanced with 1.6 % error, suggesting that the interpretation is geometrically reasonable. The interpreted shortening in the cross section is 53%, the greatest amount of lateral shortening measured in the Eola – Robberson Field.

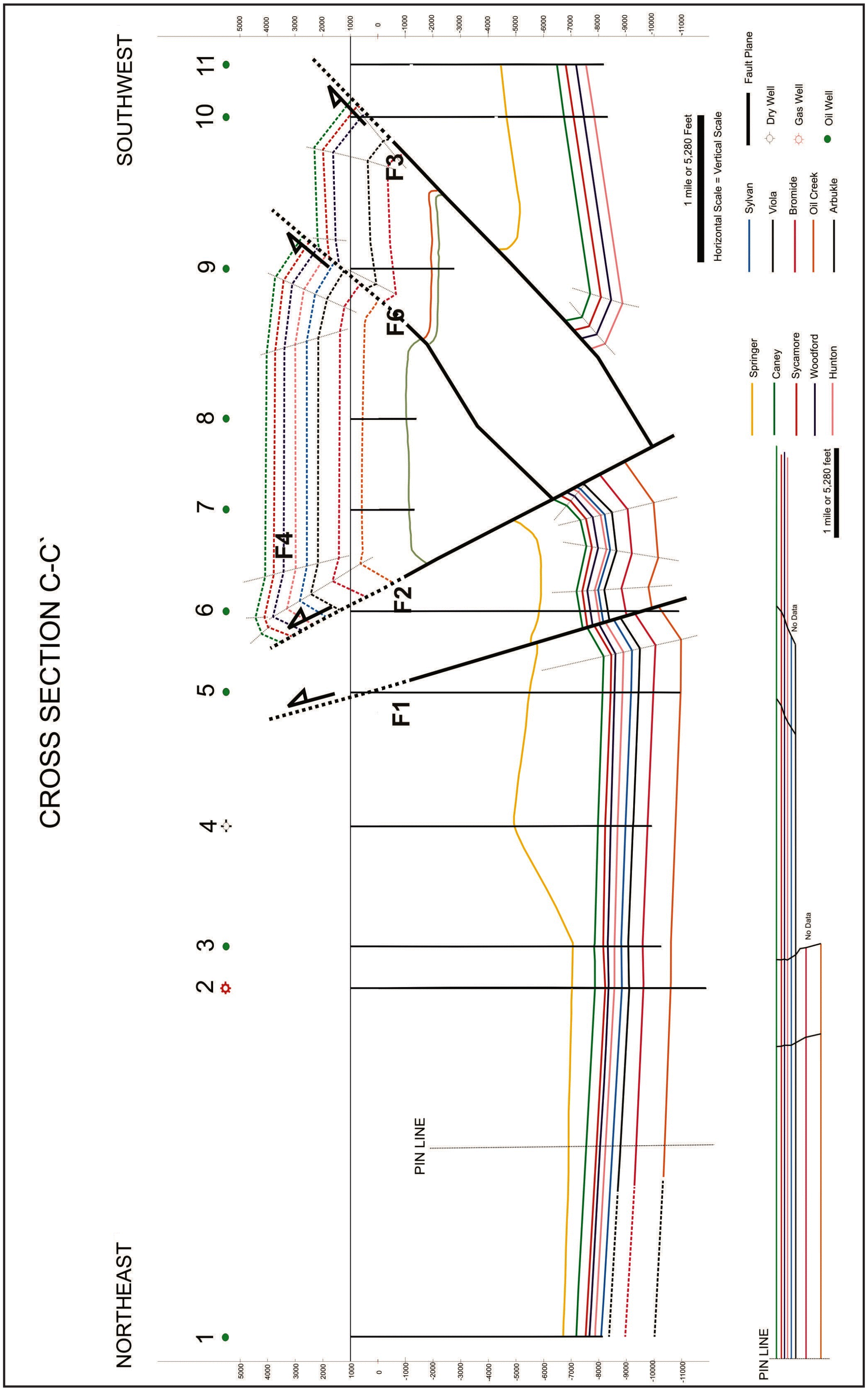

Figure 6. Cross Section C-C. API and well information can be found in Table 2.

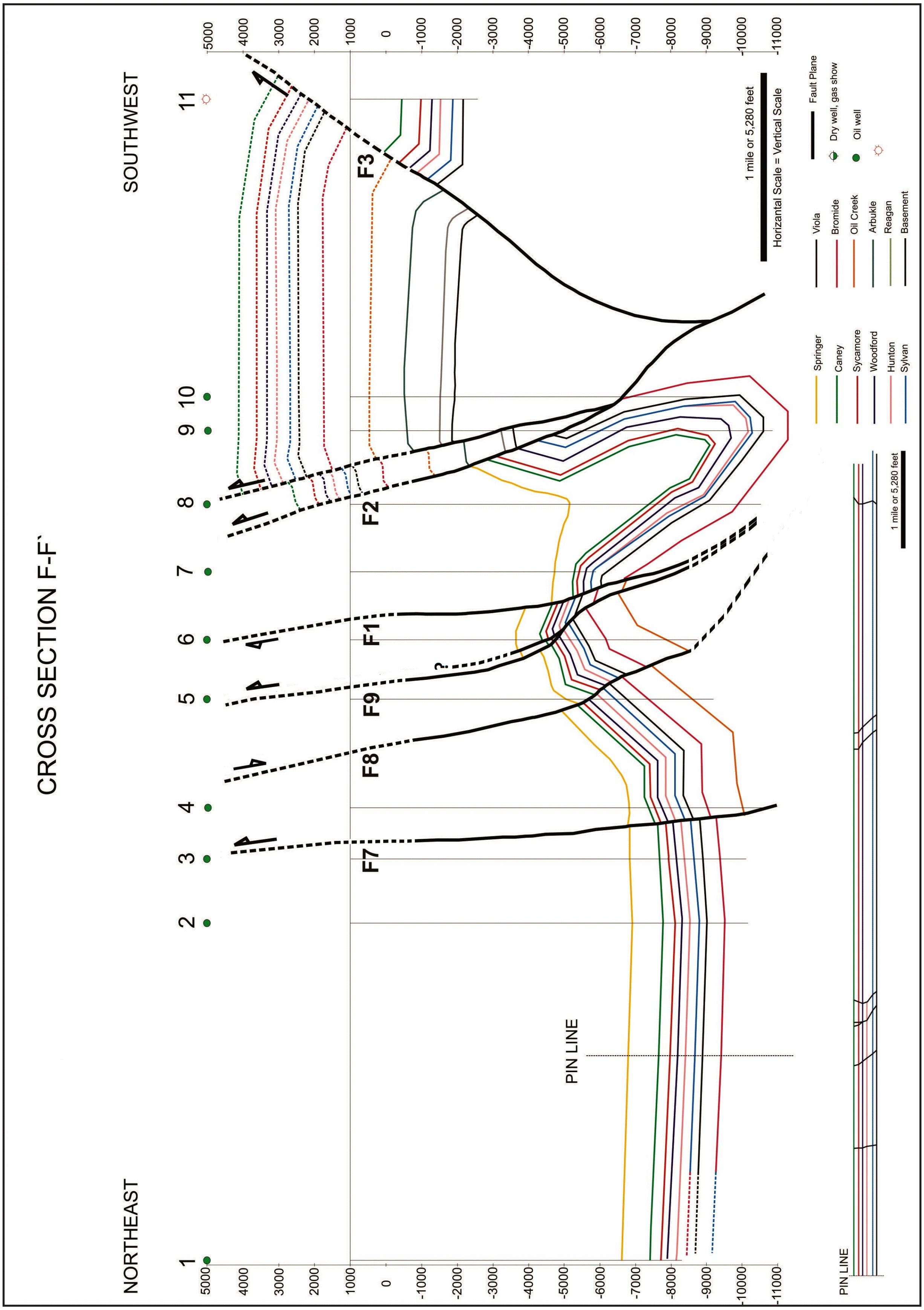

Figure 7. Cross Section F-F`. API and well information can be found in Table 2.

Discussion and Conclusions

The Eola – Robberson Field shows evidence of transpressional faulting. The northwest-southeast-striking reverse faults are major structural elements in this region that form a complex positive flower structure. The pop-up bounding faults join at depth. Fault 2 (Figure 4) is interpreted as the master, through-going fault in the region with more than 9,000 ft (2,700 m) of vertical displacement. The overall fault geometry in the Eola – Robberson Field (Figure 8) supports an interpretation of transpression. Normal faults in the field are interpreted as the tensional faults due to transpression. The best explanation for the fault geometries seen in the field can be seen from a comparison with the literature (Sanderson and Marchini, 1984). The orientation of faults in a transpressional environment in comparison to pure strike slip is shown in Figure 8. Comparison of the orientations of expected faults and folds with those found in the field support the conclusion of transpression. Our visualization of the geometry of the field is best represented in the classic work by Lowell (1985) (Figure 9).

Our work supports the interpretation by Granath (1989) and McCaskill (1998) in that the fault geometry in the field

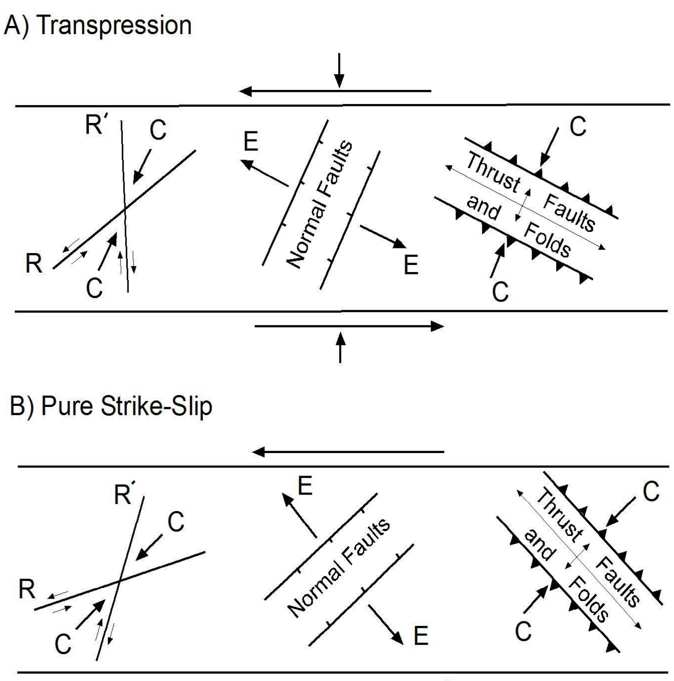

Figure 8. Geometry of faults in transpression as compared to pure strike slip (modified after Sanderson and Marchini (1984)). In the figure, C is the compressional direction in the shear zone, E is the extensional direction, R - R’ are Reidel shears associated with strike slip.

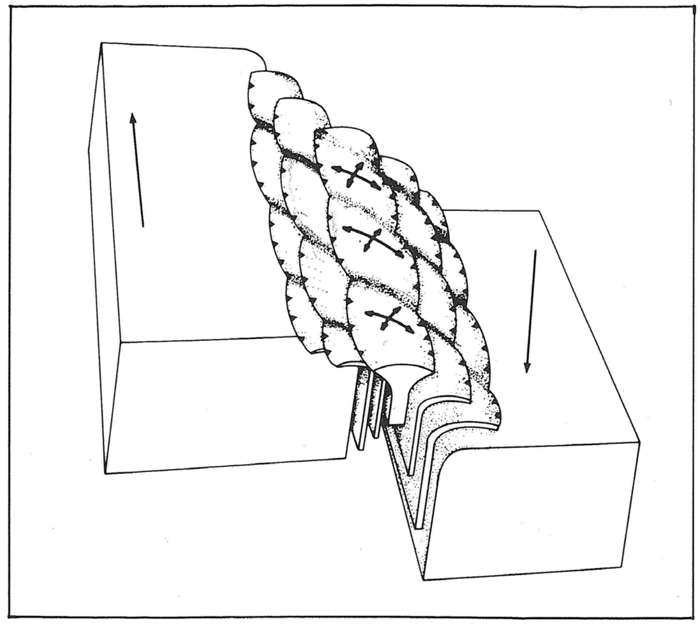

Figure 9. Visualization of transpressional system from Lowell (1985). The original figure illustrates the geometry of folds and faults seen in the Spitsbergen transpressional zone.

represents a transpressional strike-slip system. The shortening measured in the balanced cross sections suggests a greater degree of convergence in the strike-slip system than suggested by Granath (1989). In his work, he suggested a convergence angle of ~10° (see figure 2 in Carpenter and Tapp, this guidebook). Our work suggests a greater degree of convergence that needs to be investigated further to quantify the displacement field.

Our work also shows that it is possible to produce geometrically reasonable cross sections in these complex systems. The balanced cross sections presented here represent both geometrically and structurally reasonable fault geometries that provide insights into the structural style of the Eola – Robberson Field. Given the out-of-plane component of displacement, is it not possible to make any statement regarding the fault kinematics, the total strain in the field or the strain path (Dewey et al., 1998). What is clear from this research is that the structures in the field are basement controlled. The geometries of faults and displacement do not fit a thin-skinned thrust interpretation or a simple strike-slip interpretation. The best-fit interpretation is of transpression with possible reactivation of rift-related or rift-bounding faults in contraction (Williams, et al. 1989, Bonini et al., 2012). The fault geometries seen in the Eola –

Robberson are starkly similar to those shown in models of transpressional inversion (Panien et al., 2005).

This work should be viewed as a preliminary interpretation of the fault geometry. Further work is needed along strike working back toward the Arbuckle Mountains to understand the geometry and kinematics of the faults and understand the relationship between Eola – Robberson and the Arbuckle Uplift. In addition, further work is needed tracing faults into the Pennsylvanian section to understand timing and displacement on faults. We hope to continue this line of investigation with an ultimate goal of delineating the original rift-fault geometries and determine the sense of displacement and reactivation on those earlier faults in the formation of the complex structures in and around the Ardmore Basin and Arbuckle Uplift.

REFERENCES CITED

Bonini, M., Sani, F., and Antonielli, D., 2012, Basin inversion and contractional reactivation of inherited normal faults: A review based on previous and new experimental models: Tectonophysics, v. 522-523, p. 55-88.

Booth, S.L., 1981, Structural analysis of portions of the Washita Valley Fault zone, Arbuckle Mountains, Oklahoma: Shale Shaker, v. 31, p. 107-120.

Boyd, D.T., 2002, Map of Oklahoma Oil and Gas Fields: Distinguished by Coalbed Methane and Field Boundaries: Oklahoma Geological Survey Map GM-37, scale 1:500,000.

Boyd, D.T., 2008, Stratigraphic Guide to Oklahoma Oil and Gas Reservoirs: Oklahoma Geological Survey Special Publication SP 2008-1, 1 sheet.

Brown, W.G., 1984, Washita Valley Fault system - a new look at an old fault, *in* Borger, J.G., II, ed., Technical Proceedings of the 1981 American Association of Petroleum Geologists Mid-Continent Regional Meeting: Oklahoma City Geological Society, p. 68-80.

Brownlee, D.E., 1985, Stratigraphic and structural investigation of the Eola Klippe, Garvin County, Oklahoma: Shale Shaker, v. 35, p. 97-112.

Carter, D.W., 1979, A study of strike-slip movement along the Washita Valley Fault, Arbuckle Mountains, Oklahoma: Shale Shaker, v. 30, p. 79-106.

Cederstrand, J.R., 1996, Digital Geological Map of Ardmore-Sherman Quadrangle, south-central Oklahoma: U.S. Geological Survey Open-File Report 96-370.

Dahlstrom, C.D.A., 1969, Balanced cross sections: Canadian Journal of Earth Sciences, v. 6, p. 743-757.

Dewey, J.F., Holdsworth, R.E., and Strachan, R.A., 1998, Transpression and transtension zones, *in* Holdsworth, R.E., Strachan, R.A., and Dewey, J.F., eds., Continental Transpressional and Transtensional Tectonics: Geological Society of London Special Publication No. 135, p. 1-14.

Dott, R.H., 1934, Overthrusting in Arbuckle Mountains, Oklahoma: American Association of Petroleum Geologists Bulletin, v. 18, p. 567-602.

Geiser, P., 1988, The Role of Kinematics in the Construction and Analysis of Geologic Cross Sections in Deformed Terranes: Geological Society of America Special Paper 222, p. 47-76.

Granath, J.W., 1989, Structural evolution of the Ardmore Basin, Oklahoma: Progressive deformation in the foreland of the Ouachita collision: Tectonics, v. 8, p. 1015-1036.

Harding, T.P., 1990, Identification of wrench faults using subsurface structural data: Criteria and pitfalls: American Association of Petroleum Geologists Bulletin, v. 74, p. 1590- 1609.

Harlton, B.H., 1964, Tectonic framework of Eola and southeast Hoover Oil Fields and West Timbered Hills area, Garvin and Murray Counties, Oklahoma: American Association of Petroleum Geologists Bulletin, v. 48, p. 1555- 1567.

Harmon, R.E., and Tapp, B., 2001, Small-scale inversion feature on the flanks of the Ardmore Basin: Structural study of the Milroy Field: *in* Johnson, K.S., and Merriam, D.F., eds., Petroleum Systems of Sedimentary Basins in the Southern Midcontinent, 2000 Symposium: Oklahoma Geological Survey Circular 106, p. 187-190.

Harmon, R.E., Banks, R., and Suhm, R.W., 2002, Computer modeling of a small-scale inversion feature, Milroy Field, southern Oklahoma: *in* Cardott, B.J., ed., Revisiting Old and Assessing New Petroleum Plays in the Southern Midcontinent, 2001 Symposium: Oklahoma Geological Survey Circular 107, p. 37-54.

Henry, M.E., and Hester, T.C., 1995, Southern Oklahoma Province (061), *in* Gautier, D.L., Dolton, G.L., Takahashi, K.I., and Varnes, K.L., eds., 1995 National Assessment of United States Oil and Gas Gesources – Results, Methodology, and Supporting Data: U.S. Geological Survey Digital Data Series 30.

Kilic, D., 2013, Structural analysis of the Eola – Robberson Field using balanced cross sections, Garvin County, Oklahoma [M.S. thesis]: Tulsa, Oklahoma, University of Tulsa, 143p.

Lowell, J.D., 1985, Structural Styles in Petroleum Exploration: Oil and Gas Consultants International Inc., Tulsa, Oklahoma, 459p.

McCaskill, J.G., 1998, Multiple stratigraphic indicators of major strike-slip movement along the Eola Fault, subsurface –Arbuckle Mountains, Oklahoma: Shale Shaker, v. 48, p. 93-109 and p. 119-133.

Mitra, S., 1992, Balanced structural interpretations in fold and thrust belts, *in* Mitra, S., and Fisher, G.W., eds., Structural Geology of Fold and Thrust Belts, Johns Hopkins Studies in Earth and Space Sciences: Baltimore, Maryland, The Johns Hopkins University Press, p. 53-57.

Mount, V.S., Suppe, J., and Hook, S.C., 1990, A forward modeling strategy for balancing cross sections: American Association of Petroleum Geologists Bulletin, v. 74, p. 521-531.

Northcutt, R.A., and Campbell, J.A., 1995, Geologic Provinces of Oklahoma - Map and Digital Data: Oklahoma Geological Survey Open-File Report 5-95.

Panien, M., Schreurs, G., and Pfiffner, A., 2005, Sandbox experiments on basin inversion: Testing the influence of basin orientation and basin fill: Journal of Structural Geology, v. 27, p. 433-445.

Phillips, E.H., 1983, Gravity slide thrusting and folded faults in western Arbuckle Mountains and vicinity, southern Oklahoma: American Association of Petroleum Geologists Bulletin, v. 67, p. 1363-1390.

Sanderson, D.J., and Marchini, W.R.D., 1984, Transpression: Journal of Structural Geology: v. 6, p. 449-458.

Simpson-Carpenter, M.J., 2011, Structural analysis of the Sho-Vel-Tum Field and correlation to the Arbuckle Mountains using balanced cross sections, Stephens and Carter Counties, Oklahoma [M.S. thesis]: Tulsa, Oklahoma, The University of Tulsa, 165p.

Suppe, J., 1983, Geometry and kinematics of fold-bend folding: American Journal of Science, v. 283, p. 684-721.

Swesnik, R.T., and Green, T.H., 1950, Geology of Eola area, Garvin

County, Oklahoma: American Association of Petroleum Geologists Bulletin, v. 34, p. 2176-2199.

Tapp, B., 1995, Inversion model for the Structural Style of the Arbuckle region, *in* Johnson, K.S., ed., Structural Styles in the Southern Mid-continent, 1992 Symposium: Oklahoma Geologic Survey Circular 97, p. 113-118.

Williams, G.D., Powell, C.M., and Cooper, M.A., 1989, Geometry and kinematics of inversion tectonics, *in* Cooper, M.A., and Williams, G.D., eds., Inversion Tectonics: Geological Society of London Special Publication No. 44, p 3-15.

Woodward, N.B., Boyer, S.E., and Suppe, J., 1985, An outline of balanced cross sections: Notes for Short Course on Balanced Cross Sections at the Geological Society of America Annual Meeting in Orlando, Florida, November 1-2, 1985, 170p.